International Journal of Rock Mechanics & Mining Sciences 83 (2016) 174–181

Contents lists available at ScienceDirect

International Journal of Rock Mechanics & Mining Sciences

journal homepage: www.elsevier.com/locate/ijrmms

Short communication

Rock mass failure mechanisms during the evolution process of rockbursts in tunnels

Y.X. Xiao [a], X.T. Feng [a,*], S.J. Li [a], G.L. Feng [a], Y. Yu [b]

[a] State Key Laboratory of Geomechanics and Geotechnical Engineering, Institute of Rock and Soil Mechanics, Chinese Academy of Sciences, Wuhan, China
[b] Key Laboratory of Ministry of Education for Safe Mining of Deep Metal Mines, Northeastern University, Shenyang, China

ARTICLE INFO

Article history:
Received 21 May 2014
Received in revised form
25 October 2015
Accepted 8 January 2016
Available online 16 January 2016

Keywords:
Strain burst
Strain–structure slip rockburst
Evolution mechanism
Microseismic monitoring
Tunneling

1. Introduction

A rockburst is defined as damage to an excavation that occurs in a sudden or violent manner and is associated with a seismic event.[1] Rockburst is a common and serious form of engineering disaster that may happen during excavation of deeply-buried tunnels. As the depths of excavations have progressively increased, more and more cases of rockbursts in tunnels have been reported. Rockbursts can cause mechanical damage, delays to projects, and economic loss. As an example, hundreds of rockbursts occurred during the construction of the extra-long seven tunnels in the Jinping II hydropower station in China. On 28 November 2009, an extremely serious rockburst caused seven deaths and one injury, as well as the total destruction of a tunnel boring machine (TBM).

The study of rockburst evolution mechanisms is the foundation for developing theoretical and numerical models to warn of, and control, rockbursts. There has been a great amount of research carried out on the mechanisms underlying rockbursts in tunnels, including case records and laboratory tests. Ortlepp and Stacey used case records to make a significant improvement to our understanding of rockbursts and stated that strain bursts are the main form.[2,3] An on-the-spot survey of rockbursts and the failure modes of ejected rock blocks examined using a scanning electron microscope revealed that the processes causing a rockburst can be summarized as: compression cracking, compression shear cracking, bending, and breaking.[4] Early biaxial mechanical testing studies suggested that the damage produced is shear-based.[5] However, based on true triaxial laboratory tests, it was found that both tensile and shear failure can occur during rockburst evolution.[6–8] In fact, rockbursts are extremely complex phenomena influenced by several factors, *e.g.* geological conditions, the presence of groundwater, rock lithology, and the tunnel excavation itself. It is difficult to realize the actual stress path involved in the development process of rockbursts and to simulate rockburst of different types through laboratory testing. In addition, existing case studies focus on the mechanisms of rockburst occurrences. Thus, how to obtain direct evidence on the evolution mechanisms behind rockbursts remains an unresolved problem.

Microseismic (MS) monitoring is important for understanding the *in situ* process of rock mass failure associated with rockbursts.[9,10] The process of rockburst evolution can be seen as a series of rock mass failure events related to MS events. This means that if we can identify the types of rock mass failure events involved in the process of development of rockbursts (tensile, mixed, or shear), the rockburst evolution mechanisms can be obtained directly. Based on such MS information, methods involving energy ratios and moment tensor analysis have been widely used to judge the type of rock mass failure occurring. A large number of MS monitoring results have indicated that the energy ratios of tensile failure events are much smaller than those for shear failure events.[11–14] To study the characteristics of the type and crack plane

* Corresponding author.
E-mail addresses: xtfeng@whrsm.ac.cn, xia.ting.feng@gmail.com (X.T. Feng).

http://dx.doi.org/10.1016/j.ijrmms.2016.01.008

of rock mass failure, the moment tensor analysis method was introduced and later improved.[15,16] However, the applicability of these two methods still required verification using real-time MS monitoring of tunnel engineering projects.

The aim of the study reported here is to explore the evolution mechanisms of rockbursts in tunnels. For this purpose, a comprehensive method of judging the type of rock mass failure occurring during rockburst evolution is proposed based on real-time MS information. The features and evolution mechanisms behind a series of rockburst cases of different types are presented. At the same time, the effect of stiff structure on the rockburst evolution process is also discussed.

2. Microseismic monitoring of rockburst evolution processes in tunnels

2.1. Microseismic monitoring in the tunnels of Jinping II

In situ MS monitoring was conducted in the four headrace tunnels and a drainage tunnel of the Jinping II hydropower station in China (with a total length of 12.4 km) to study the rockburst evolution process and warn of rockburst risk. The diameters of the headrace and drainage tunnels are 13 and 7.3 m, respectively. The burial depth of these tunnels varies from 1900 to 2525 m. Detailed information on the MS monitoring zone, cross sections, and geology of the Jinping II tunnels can be found elsewhere in the literature.[9,17] Several working faces were setup in these tunnels to speed up the construction process and one or two six-channel MS acquisition units were placed at each working face (see Fig. 1). Two groups of sensors were installed behind each workface and these were moved forward progressively as the tunnel face advanced. The monitoring program and related sensor layout have already been reported by Chen et al.[18]

In contrast to large-scale MS monitoring in mines, MS monitoring in tunnels presents two obvious differences: (i) as the sensors are repeatedly moved forwards, the distance between the MS sources and sensors is usually small (less than 150 m). This means that most failure events can only be recorded by the sensors near to where an event occurs (referred to as 'near sensors') and cannot trigger sensors in other tunnels (referred to as 'far sensors'), as shown in Fig. 1. For example, 354 of the 471 MS events occurring in April 2011 were just recorded by near sensors. (ii) The failure events are basically outside the sensor array.

2.2. Description of rockbursts in tunnels

In terms of development mechanism and effect of geological structure, there are two main types of rockbursts during tunnel excavation: strain bursts and strain–structure slip rockbursts.[9,10] The main factor controlling both of these rockbursts is the same: high geo-stress. The latter is also commonly affected by the presence of stiff structures. Typically, strain bursts occur in regions with hard rock masses that are intact and with few discontinuities. The rock faces of the explosion pits generated by strain bursts are typically fresh. The shapes of the explosion pits are often nested, or V-shaped (see Fig. 2a). Strain–structure slip rockbursts occur in zones with hard rock masses containing sporadic stiff structures. Most of these stiff structures are closed, dry, without filling, and of low ductility. At the same time, the number of stiff structures is usually not greater than two (or two sets), as shown in Fig. 2b and c.

The rockburst cases considered here derive from the headrace tunnels of the Jinping II hydropower station in China. The selected rockburst cases satisfy the following three requirements: (i) the rockburst grade is moderate or intense; (ii) continuous MS information is available throughout the rockburst development process; and (iii) clear photographs were taken of the resulting explosion pit. The grade of the rockburst is determined according to the depth of the explosion pit: for a moderate rockburst this is 0.5–1 m and for an intense one it is 1–3 m.

According to the type of rockburst and number of stiff structures in the rockburst zone, three different kinds of rockbursts can be identified: (1) strain bursts, (2) strain–structure slip rockbursts with the development of a single stiff structure (or a single set thereof), and (3) strain–structure slip rockbursts with the development of two stiff structures (or two sets thereof). The numbers of these three different kinds of rockburst cases is 6, 7, and 5, respectively, based on the aforementioned selection principles.

3. Methods of evolution mechanism analysis for rockbursts in tunnels

3.1. The energy ratio method

In this method, the radiated MS energies of rock mass failure events are calculated using seismogram processing software provided by Integrated Seismic System (ISS). The calculation follows that of Mendecki et al.[19] by use of the formula:

$$E_{P,S}=\frac{8}{5}\pi\rho v_{P,S}R^2\int_0^{t_s}\dot{u}_{corr}^2(t)dt \tag{1}$$

where $E_{P,S}$ is the P- or S-wave energy, ρ is the rock density, $v_{P,S}$ is the P- or S-wave velocity, R is the distance from the source, t_s is the duration, and $\dot{u}_{corr}^2(t)$ is the square of the far-field-corrected radiation pattern of the velocity pulse.

The ratio of the S- and P-wave energies (E_S/E_P) can be used to judge the type of focal mechanism responsible for generation of an MS event. It is generally accepted that E_S/E_P values associated with rock mass failure events involving tensile failure are less than 10.[11,12] If the rock mass failure process can be viewed as involving shear failure, then E_S/E_P is greater than 20.[13,14] Thus, the energy ratio criteria can be summarized as:

$$\begin{cases} E_S/E_P<10 & \text{Tensile failure} \\ 10 \le E_S/E_P \le 20 & \text{Mixed failure} \\ E_S/E_P > 20 & \text{Shear failure} \end{cases} \tag{2}$$

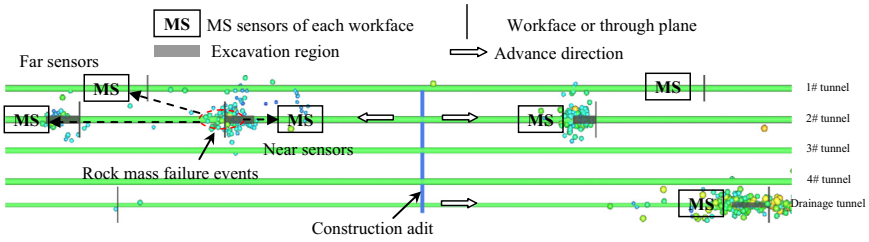

Fig. 1. Schematic representation of the microseismic monitoring system used in the headrace tunnels at the Jinping II hydropower station in China.

(a)

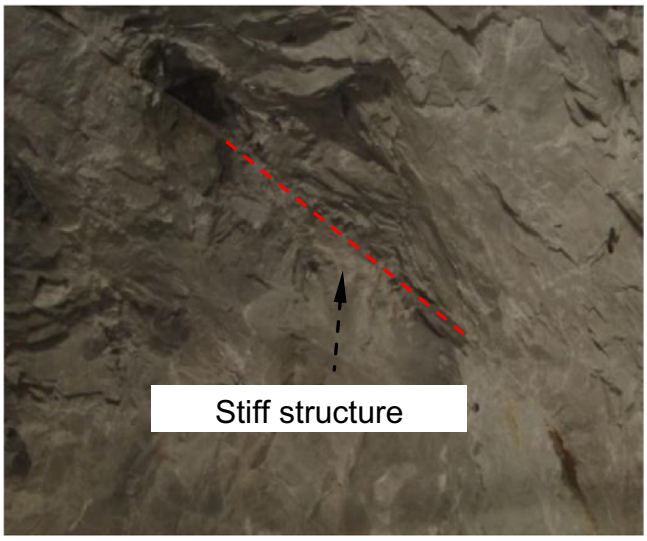

(b)

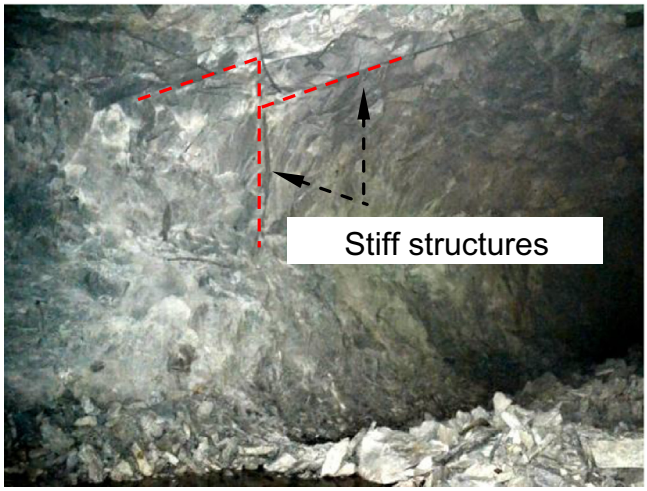

(c)

Fig. 2. Typical rockbursts in tunnels: (a) an intense strain burst which occurred on 18 August 2010, (b) a moderate strain–structural slip rockburst with the development of one stiff structure which occurred on 13 December 2010, and (c) an intense strain–structural slip rockburst with the development of two sets of stiff structures which occurred on 10 August 2010.

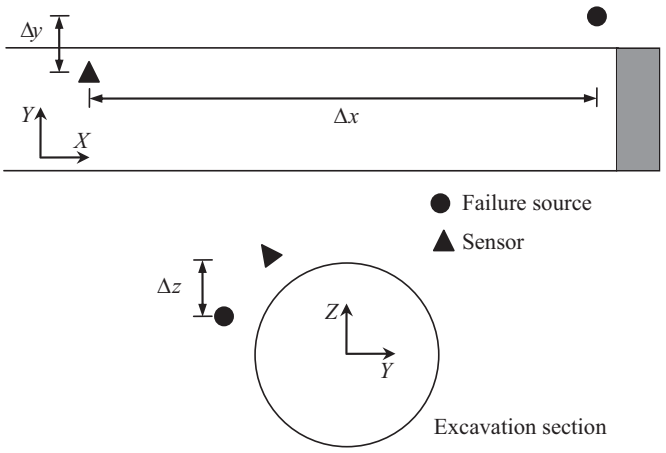

Fig. 3. The spatial relationship between a failure source and a sensor in a tunnel.

3.2. Moment tensor analysis

Ming et al. derived an improved method of moment tensor analysis to judge the type of rock mass failure occurring in deeply buried tunnels.[20] The moment tensor M_{ij}, is a second-order symmetric matrix, whose components are given by, [21]

$$u_P = \frac{\gamma_i \gamma_j}{4\pi\rho v_P^3 R} M_{ij} \tag{3}$$

here u_p is the far-field displacement of the P-wave, and the γ factors represent the cosines of the angles between a ray spreading from the source to the sensor and each coordinate axis: $\gamma_1 = \Delta x/R$, $\gamma_2 = \Delta y/R$, and $\gamma_3 = \Delta z/R$, where Δx, Δy, and Δz are the projected distances between the source and sensor in the X-, Y-, and Z-directions, respectively, as shown in Fig. 3.

During real-time MS monitoring in tunnels, Δx is often much greater than Δy and Δz. At times, the ratio of Δx and Δy (or Δz) can reach up to 100, so the value of M_{22} (or M_{33}) will be 10,000 times that of M_{11} according to Eq. (3). This will cause the calculation of scalar value of moment tensor relies on one of its components heavily. Accordingly, the resulting moment tensor may be inaccurate.[20] A coordinate transformation, however, will not change the eigenvalue of the moment tensor, and will therefore not influence the subsequent judgment of the failure type. Therefore, an appropriate rotation of the coordinate axes is carried out to reduce the differences among the three direction cosines. A large number of moment tensor calculations indicate that an ideal result for moment tensor can be obtained if the differences between the three direction cosines are less than 10.

The elements of the moment tensor can be decomposed into three parts: an isotropic part (ISO), a double-couple part (DC), and a linear vector dipole (CLVD) component. This decomposition can be interpreted in the mining environment.[12,15] The ISO part of the moment tensor is not usually considered in seismology and for mining earthquakes, where fault motion of the shear type is considered to be the major causal mechanism. The use of shear (DC) and tensile (CLVD+ISO) contributions to MS and acoustic emission (AE) events is sometimes adopted,[14,22–23] although this decomposition does not, in general, represent failure. Thus, the percentage shear component:

$$DC\% = 100 * M^{DC} / \left(|M^{DC}| + |M^{CLVD}| + |M^{ISO}| \right),$$

can be used to judge the type of rock mass failure occurring. The set of criteria in this case becomes:

$$\begin{cases} DC\% \le 40 & \text{Tensile failure} \\ 40 < DC\% < 60 & \text{Mixed failure} \\ DC\% \ge 60 & \text{Shear failure} \end{cases} \quad (4)$$

3.3. Method of P-wave development

It is well-known that when elastic waves are released as a result of failure, that different types of rock mass failure events produce waves with different characteristic wave motions. Based on the MS monitoring data from the Jinping II hydropower station, a method of evaluating the type of failure using the development of P-waves has been established by Feng et al.[17] The P-wave development parameter, P_D, is defined as:

$$P_D = \sum_{i=1}^{N} A_P^i / A_M^i \quad (5)$$

where N is the number of sensors triggered when the MS event occurred, and A represents the amplitude of the P-wave. The amplitude A_P^i is that of the P-wave's first motion in the waveform, as recorded by the i-th triggered sensor, and A_M^i is the maximum amplitude recorded in the waveform at the i-th triggered sensor. The criteria used with this measure are:

$$\begin{cases} P_D \ge 0.047 & \text{Tensile failure} \\ P_D < 0.047 & \text{Shear failure} \end{cases} \quad (6)$$

It must be pointed out that P_D is calculated from the time-domain waveform recorded using a velocity geophone. If the triggered sensors are accelerometers, then the numerical integral of the acceleration–time curve in the time domain should be evaluated to restore the original velocity–time curve of the MS wave.

3.4. Applicability of the three methods in tunnels

During the entire MS monitoring program, 65 MS events (with seismic energy equal to or exceeding 2.4×10^5 J) were recorded by both near and far sensors under MS monitoring conditions similar to those shown in Fig. 1. Based on this information, the types of failure events involved were judged using the energy ratio, moment tensor analysis, and P-wave development methods. Most of the assignments were consistent with each other. In particular, the MS events associated with rockburst occurrence due to obvious shear failure were all essentially judged to be due to shear failure by all three methods. Therefore, these consistent results can be taken as true allocations of the types of failure associated with these MS events. It should also be noted that mixed-type assignments depend on the first two methods only.

If judgment is made using just the information from the near sensors alone, then the coincidence rate between the three methods falls to less than 40%. As mentioned before, most of the MS events were recorded by just the near sensors. Thus, solving the problem of how to appropriately judge the rock mass failure type based only on information from near sensors is key to investigating rockburst evolution mechanisms. By comparing the judgments made by the three methods using just the information from near sensors with the confirmed type of MS event (based on all data), the applicability of the three methods with respect to near-sensor information can be analyzed. The findings are summarized as follows[17]:

(1) if the type of failure is shear or mixed, the energy ratio method has a good chance of being correct (the accuracy reached 73% and 100%, respectively). However, the precision rate of this method with respect to tensile failure was only 33%. The start of the S-wave is often considered as the end of the P-wave, and part of the P-wave is combined into the region of the S-wave in the MS waveforms recorded by the near sensors. The calculated P-wave energy is only part of the real value, and this will make the calculated value of E_S/E_P larger than its true value. This is why the tensile rock mass failure events could not be interpreted accurately using the energy ratio method.
(2) The moment tensor method judged tensile and mixed failure events quite well (with precisions exceeding 90% and 70%, respectively). However, the accuracy with respect to shear failure was less than 30%. The reason for this is that the near sensors were within the same quadrant of the focal sphere. Under such conditions, the excitation matrix can be singular and this will seriously affect the accuracy of shear failure judgments. The inclusion of information from far sensors can, of course, remedy this situation quite effectively.
(3) The accuracy of the P-wave development method with respect to tensile and shear failure events was about 90% in both cases. At the same time, the results obtained using this method showed good consistency when information from near and far sensors was used separately. The P-wave development method is easy to understand and implement. However, this method cannot be used to judge mixed-mode failure and is greatly influenced by the denoising of MS waveforms.

3.5. Comprehensive method

According to the advantages and disadvantages of the three methods discussed above, a new, more comprehensive method is proposed. The method uses the DC% component of the moment tensor and the P-wave development factor of an MS event as its main judgment parameters; the energy ratio is also used as an auxiliary decision parameter. The implementation process of this new method can be divided into five steps:

(1) the type of rock mass failure event is independently judged according to the moment tensor analysis and P-wave development methods.
(2) If the judgment results from the two parameters are the same: i.e. tensile or shear, then this consistent result can be taken as the failure type.
(3) Otherwise, the failure event is more likely to be of mixed or shearing type. Then, the energy ratio method is used to identify the failure type.
(4) A consistent result between the energy ratio method and one of the other two methods can be taken as representing the final judgment of the failure type.
(5) In rare cases, the results of these three methods may all be different. In this case, failure is finally considered to be of mixed type.

According to a large number of failure type assignments, the types of most rock mass failure events during rockburst evolution can be determined using the aforementioned first two steps.

4. Results

4.1. Verification of the analysis method

The mechanisms of the rock mass failure events related to the MS events in the zone and surrounding region of the rockbursts (extending to 1.5 times the excavation diameter on both sides of the explosion pit boundary) were analyzed using the new method. Subsequently, the type of rock mass failure occurring at different

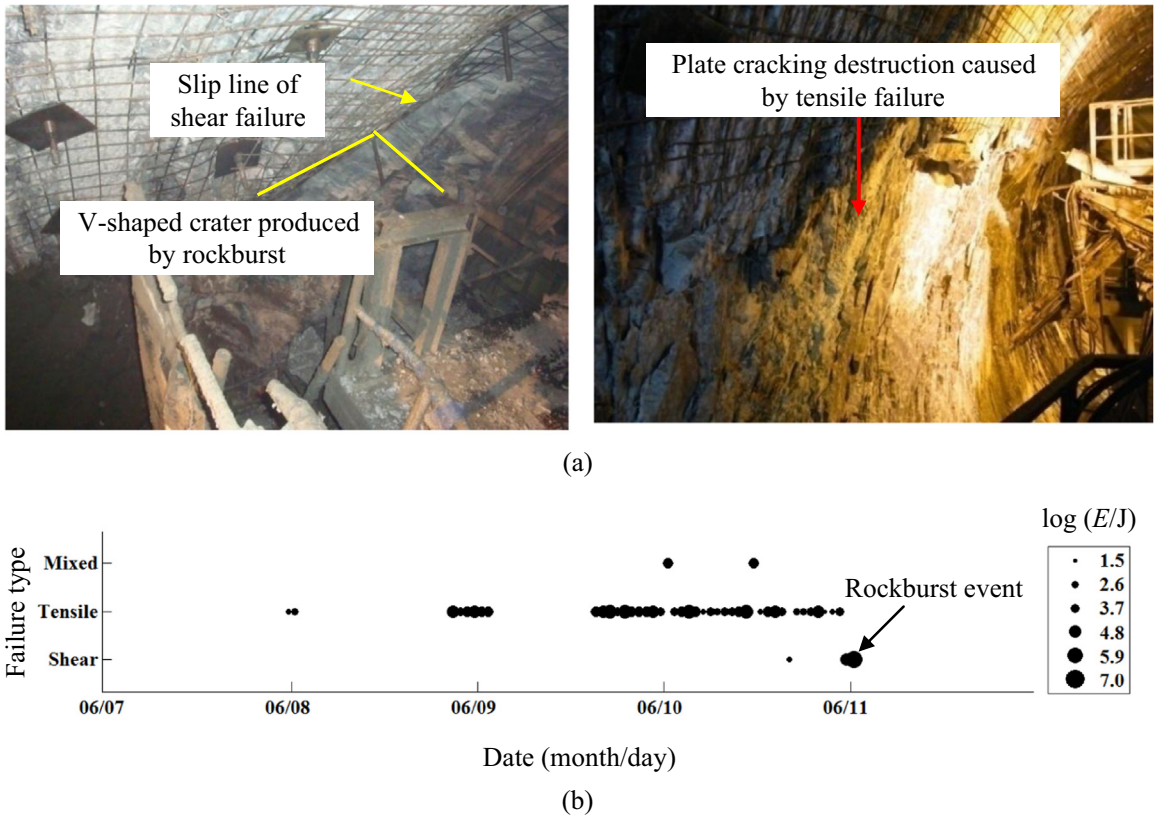

Fig. 4. Details of the rockburst case used to illustrate the proposed comprehensive method of judging failure type: (a) photographs of the surrounding rock failure produced by the rockburst, and (b) the change in the type of failure occurring during the development of the rockburst.

times in the rockburst development process could be found. The macro-failure characteristics of the rockburst pit, explosive rock blocks, and rock mass around the rockburst zone all reflect the evolution mechanism of the rockburst. Accordingly, the reliability of the proposed method in judging the rock mass failure type can be checked. More than 10 rockburst cases were analyzed to verify the proposed analysis method – one such case is presented in detail to illustrate how the work was carried out.

At about 00:30 on 11 June 2010, an intense rockburst occurred in the south wall side of the 3# tunnel (at chainage 11+040 to 11+054) while it was under TBM excavation. The explosion pit, with a maximum depth of 1.2 m, had a V-shaped appearance. The upper boundary of the rockburst pit was controlled by a stiff structure and presented a scarp-shaped appearance (Fig. 4a). The mechanism of occurrence of the rockburst can be deduced by analyzing the failure characteristics, as we now summarize:

(i) Plate cracking was apparent in the sidewall and floor near the rockburst zone (see Fig. 4a). The surrounding rock mass will also have the same failure feature in its rockburst zone. This phenomenon is due to stress-induced splitting failure related to tensile failure. At the same time, most of the explosive rock blocks are massive and tensile cracks with 'fish-shaped' patterns can be seen. The majority of the failure features of this rockburst are thus indicative of a tensile failure mechanism.

(ii) As shown in Fig. 4a, striations caused by shear sliding appear on the surface of the rock of the explosion pit. At the same time, the form of the explosion pit is controlled by a stiff discontinuity and an obvious shear slide-line can be seen. This means that the rockburst occurred in the form of a shear failure.

The rock mass failure types occurring during the evolution of the rockburst based on the new method are as shown in Fig. 4b. (Each circle represents a rock mass failure event and its size represents the logarithm of the radiated seismic energy of the MS event.) The last event is related to the rockburst occurrence. It can be seen that most of the rock mass failure events are tensile in nature but the ultimate failure mode of the rockburst is shear. The implied mechanism of evolution of this rockburst, as shown in Fig. 4, is thus consistent with that revealed by the macro-failure characteristics. Thus, the proposed comprehensive method appears to be reliable.

4.2. Rock mass failure evolution and 'big' events

Using the newly established comprehensive method, the type of rock mass failure occurring during the development of eighteen rockbursts of different types was identified. The evolution of these rockbursts can be summarized as follows.

During a strain burst, tensile failure predominates and there are very few shear or mixed failure events. This is shown in Fig. 5a. The failure events occurring are all tensile before the strain burst happens and only the occurrence of the ultimate rockburst itself is caused by shear failure.

In the evolution of a strain–structure slip rockburst, a few small tensile failure events appear at first. Then, some shear, mixed, and tensile failure happens alternately. The rockburst ultimately occurs in the form of a shear failure (see Fig. 5b and c).

The behavior of rockbursts with different numbers of stiff structures present do not exhibit significant differences – the main type of rock mass failure occurring remains tensile, as before (see Fig. 5b and c).

The first appearance of an MS event in the rockburst zone can be considered as the starting time for the subsequent rockburst

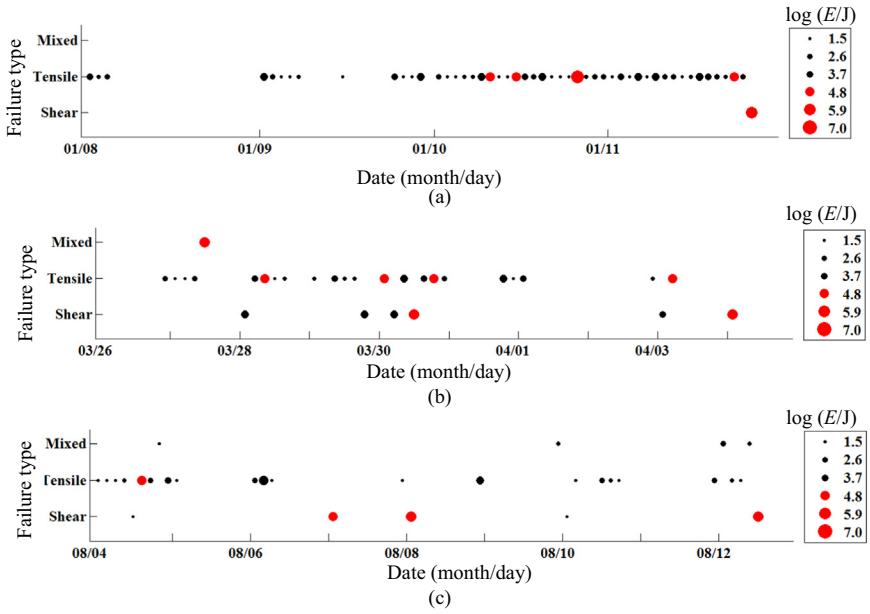

Fig. 5. The type of failure events occurring during rockburst evolution for: (a) an intense strain burst which occurred on 11 January 2011, (b) a moderate strain–structural slip rockburst with the development of one stiff structure which occurred on 4 April 2011, and (c) an intense strain–structural slip rockburst with the development of two stiff structures which occurred on 12 August 2011.

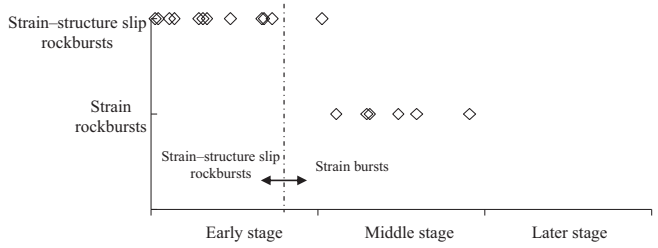

Fig. 6. The onset of occurrence of big events occurring during rockburst development.

evolution and the occurrence of the rockburst marks the end of the development process. Rockburst evolution can be divided into three roughly equal stages in the time domain: the early, middle, and late stages. If the logarithm of the radiated seismic energy is not less than 4.8, the failure event is classified as a 'big' event. It can be seen (Fig. 5) that there are 'big' events involved in the development processes of all the rockburst cases studied. However, the first time such a 'big' event occurs is different depending upon the type of rockburst involved. More specifically, big events occur earlier on in the development process of strain–structure slip rockbursts compared to their occurrence in strain bursts. As shown in Figs. 5a and 6, the big events occurring appear in the middle and later stages of strain burst development. However, for most strain–structure slip rockbursts, the big events first occur in the early stages (Figs. 5b, c, and 6).

4.3. Failure type proportions

The proportions of the different failure types occurring in each class of rockburst were further studied. In strain bursts, the proportion of tensile rock mass failure events is no less than 92.5%. The average proportions of mixed and shear failure events, on the other hand, are only 1.2% and 3.7%, respectively.

If a rockburst zone develops one, or a single set of, stiff structures (resulting in a strain–structure slip rockburst), then the maximum proportion of tensile failure events decreases to less than 90%. In addition, the average proportions of mixed and shear failure events are three times greater than in strain bursts. For strain–structure slip rockbursts with two, or two sets of, stiff structures, the minimum proportion of tensile failure is only 55.6%. At the same time, the average proportions of mixed and shear failure events reaches 13.8% and 18.1%, respectively. The average proportions of each failure type occurring in the abovementioned rockburst evolution processes are shown in Fig. 7. It can be seen that the proportion of tensile failure events shows a tendency to decrease as the number of stiff structures increases. On the other hand, the proportions of mixed and shear failure events increase. In addition, for most of the rockburst cases analyzed here, the proportion of tensile failure events is greater than 70% and that of shear failure events is less than 20%.

5. Discussion

The new method proposed here is suitable for determining what type of rock mass failure should be associated with MS events that occur during rockburst evolution in tunnels. There are two points to bear in mind: (i) most rock mass failure events

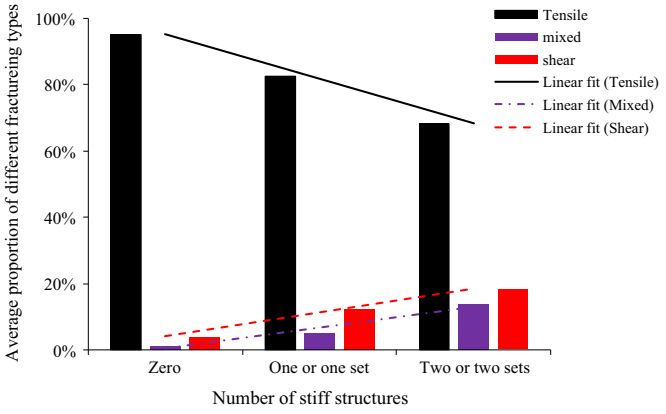

Fig. 7. The effect of the number of stiff structures on the frequency of occurrence of different failure types during rockburst development in tunnels.

occurring in the process of evolution of strain bursts and strain–structure slip rockbursts are tensile in nature (see Figs. 5 and 7); and (ii) the three methods of mechanism analysis all have their limitations (as discussed previously). The DC proportion of the moment tensor and P_D factor for the failure event are taken as the main parameters to use in the judgment process. This is because these methods have good accuracy with respect to tensile failure. The E_S/E_P value of a failure event usually only needs to be calculated to judge mixed and shear failure events. The new method can be applied to analyze the mechanism of rock mass failure occurring during tunnel excavation using the kind of MS monitoring shown in Fig. 1. However, if the MS monitoring conditions change, the suitability of the method of mechanism analysis must be rechecked.

Regardless of the type of rockburst (strain burst or strain–structure slip), the rockburst evolution mechanism is rich in tensile failure events. For deeply buried tunnels, the surrounding rock mass is usually in a state of high triaxial geo-stress. Unloading effects due to tunnel excavation will result in adjustment and redistribution of this three-dimensional *in situ* stress state. Accordingly, tangential stress gradually increases. As a result, stress-induced cracks with the orientation of the tangential stress will continue to form in the rockburst zone with integrated rock mass. This explains why the macro-failure evidence in and near the rockburst zone often takes the form of plate splitting,[3,7] as shown in Fig. 4a. These stress-induced cracks are related to the series of tensile failure events recorded *via* MS monitoring.[11] The blocks ejected as a result of rockbursts usually exhibit signs of transgranular brittle fractures and tension destruction as well.[2]

The presence of stiff structures has a strong effect on the rockburst evolution process. The proportion of shear and mixed type failure events occurring during the evolution of a strain–structure slip rockburst is usually greater than in strain bursts. This is because a sudden slip or shear may occur along any stiff structure appearing in the failure zone of the rockburst (or on the rupture surfaces of splitting plates) due to the combined effect of the stiff structure itself and tangential stress.[24] Correspondingly, we found that mostly tensile failure events occurred during the development processes of twenty-one strain bursts.

In terms of microseismic activity, 'big' events with high seismic energy appear earlier on during the evolution of a strain–structure slip rockburst compared to in strain bursts. For strain bursts, large-scale failure (like that occurring during a big event) can only happen when the tensile cracks have developed to a certain degree. A stiff structure, however, can hinder the stress regulation process from the surface to deeper regions of the surrounding rock mass. This causes stress concentration and energy accumulation in the rockburst zone.[25] This leads to acceleration of the failure processes in the surrounding rock mass and so shear failure (and accompanying high-energy release) is more likely to occur with stiff structures.

6. Conclusions

A comprehensive method for judging the type of rock mass failure occurring during rockburst evolution in tunnels based on MS information recorded in real-time has been presented. The proposed method was applied to three types of rockburst cases occurring in the tunnels of the Jinping II hydropower station which are subject to a maximum overburden of 2525 m.

The new method, which uses decomposed parts of the moment tensor and the P-wave development factor of the MS event to form the main judgment criteria (and energy ratio as an adjunct measure), can provide a reliable estimate of the rock mass failure type occurring during rockburst evolution. The results indicate that most of the failure events occurring during the development of a strain burst are tensile in nature. Strain–structure slip rockburst development begins with a few small tensile failure events at first. Then, alternating shear, mixed, and tensile failure events occur. Moderate and intense rockbursts commonly occur, ultimately, in the form of shear failure.

As the number of stiff structures present increases, tensile events tend to decrease in frequency and the proportion of shear and mixed events increases. However, tensile failure remains the main failure type occurring during development of these kinds of rockbursts in tunnels.

'Big' events occur during rockburst development. However, the first occurrence of these kinds of events depends on the rockburst type. Big events can appear in the early stages of development of strain–structure slip rockbursts, whereas, in strain burst development, they usually only feature in the middle and later stages of the evolution process.

When warning of the risk of a rockburst happening, it is necessary to consider the classification of the rockburst as different types of rockburst have different mechanisms driving them. Based on real-time MS monitoring information, two equations with six variables have been developed to warn of strain bursts and strain–structure slip rockbursts.[9] The warning predictions are more accurate when the rockburst type is classified. During the MS monitoring program carried out at the Jinping II hydropower station, the new rockburst warning method achieved an accuracy of up to 88%.

Acknowledgments

The authors gratefully acknowledge financial support from The National Natural Science Foundation of China (Grant nos. 11232014, 11355001 and 51509244). We also thank Prof. Chen Bingrui, Prof. Zhou Hui, Wu Shiyong, Wang Jimin, Zeng Xionghui, and Dr. Yan Wenfa who helped with the microseismicity monitoring program in the headrace and water drainage tunnels of the Jinping II hydropower station. We also highly appreciate the helpful suggestions and comments from Prof. Zhang Haijiang, an anonymous Associate Editor, and the manuscript reviewers who all helped to get this work into its final form.

References

1. Kaiser PK, Tannant DD, McCreath DR. *Canadian Rockburst Support Hand Book.* Sudbury, Ontario: Geomechanics Research Centre, Laurentian University; 1996.
2. Ortlepp WD, Stacey TR. Rockburst mechanisms in tunnels and shafts. *Tunn Undergr Space Technol.* 1994;9:59–65.
3. Ortlepp WD. The behaviour of tunnels at great depth under large static and dynamic pressures. *Tunn Undergr Space Technol.* 2001;16:41–48.
4. Hou ZS, Gong QM, Sun ZH. Primary failure types and their failure mechanisms of deep buried and intact marble at Jinping II hydropower station. *Chin J Rock Mech Eng.* 2001;30:727–732 in Chinese.
5. Hoek E, Brown ET. *Underground Excavation in Rock.* Beijing: Metallurgical Industry Press; 1986.
6. Gong QM, Yin LJ, Wu SY, Zhao J, Ting Y. Rock burst and slabbing failure and its influence on TBM excavation at headrace tunnels in Jinping II hydropower station. *Eng Geol.* 2012;124:98–108.
7. Gu MC, He FL, Chen CZ. Study on rockburst in Qingling tunnel. *Chin J Rock Mech Eng.* 2002;21:1324–1329 in Chinese.
8. He MC, Miao JL, Feng JL. Rock burst process of limestone and its acoustic emission characteristics under true-triaxial unloading conditions. *Int J Rock Mech Min Sci.* 2010;47:286–298.
9. Feng GL, Feng XT, Chen BR, Xiao YX, Yu Y. A microseismic method for dynamic warning of rockburst development processes in tunnels. *Rock Mech. Rock Eng.* 2015;48:2061–2076.
10. Feng XT, Chen BR, Li SJ, et al. Studies on the evolution process of rockbursts in deep tunnels. *J Rock Mech Geotech Eng.* 2012;4:289–295.
11. Cai M, Kaiser PK, Martin CD. A tensile model for the interpretation of microseismic events near underground openings. *Pure Appl Geophys.* 1998;153:67–92.

12. Gibowicz SJ, Young RP, Talebi S, Rawlence DJ. Source parameters of seismic events at the underground research laboratory in Manitoba, Canada-scaling relations for events with moment magnitude smaller than -2. *Bull Seismol Soc Am.* 1991;81:1157–1182.
13. Mcgarr A. Some applications of seismic source mechanism studies to assessing underground hazard. In *Proceedings of Rockburst and Seismicity in Mines, Symposium Series 6*, South Africa Institute of Mining and Metallurgy 1; 1984: 199–208.
14. Boatwright J, Fletcher JB. The partition of radiated energy between P and S waves. *Bull Seismol Soc Am.* 1984;74:361–376.
15. Feignier B, Young RP. Moment tensor inversion of induced microseismic events: evidence of non-shear failures in the $-4 < M < -2$ moment magnitude range. *Geophys Res Lett.* 1992;19:1503–1506.
16. Baker C, Young RP. Evidence for extensile crack initiation in point source time-dependent moment tensor solutions. *Bull Seismol Soc Am.* 1997;87:1442–1453.
17. Feng XT, Chen BR, Zhang CQ, Li SJ, Wu SY. *Mechanism, Warning and Dynamic Control of Rockburst Development Processes* Beijing: Science Press; 2013 in Chinese.
18. Chen BR, Feng XT, Li QP, Luo ZR, Li SJ. Rock burst intensity classification based on the radiated energy with damage intensity at Jinping II hydropower station, China. *Rock Mech Rock Eng.* 2015;48:289–303.
19. Mendecki AJ, Lynch RA, Malovichko DA. Routine seismic monitoring in mines. *VNIMI Seminar on Seismic Monitoring in Mines*; 2007.
20. Ming HJ, Feng XT, Chen BR, Zhang CQ. Analysis of rockburst mechanism for deep tunnel based on moment tensor. *Rock Soil Mech.* 2013;34:163–173 in Chinese.
21. Strelitz RA. Moment tensor inversions and source models. *Geophys J R Astron Soc.* 1978;52:359–364.
22. Ohtsu M. Simplified moment tensor analysis and unified decomposition of acoustic emission source: application to in situ hydrofracturing test. *J Geophys Res.* 1991;96:6211–6221.
23. Zhao P, Kühn D, Oye V, Cesca S. Evidence for tensile faulting deduced from full waveform moment tensor inversion during the stimulation of the Basel enhanced geothermal system. *Geothermics.* 2014;52:74–83.
24. Zhou H, Meng FZ, Zhang CQ, Hu DW, Yang FJ, Lu JJ. Analysis of rockburst mechanisms induced by structural planes in deep tunnels. *Bull. Seismol. Soc. Am.* 2015;74:1435–1451.
25. Zhang CQ, Feng XT, Zhou H, Qiu SL, Wu WP. Case histories of four extremely intense rockbursts in deep tunnels. *Rock Mech Rock Eng.* 2012;45:275–288.